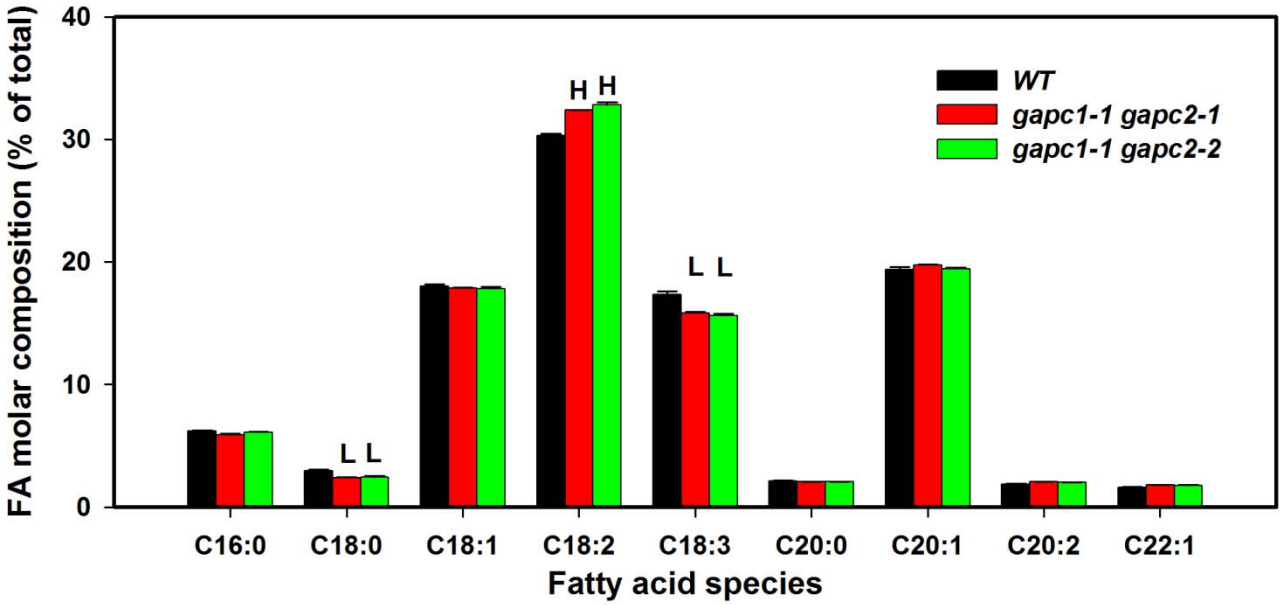

Supplemental Figure 1. Fatty acid composition of *GAPC* double knockouts compared to WT. Fatty acid composition was calculated as mol%. Values are means ± SD (n = 3). H and L indicate significantly higher and lower than WT (Student's *t*-test, P < 0.05).

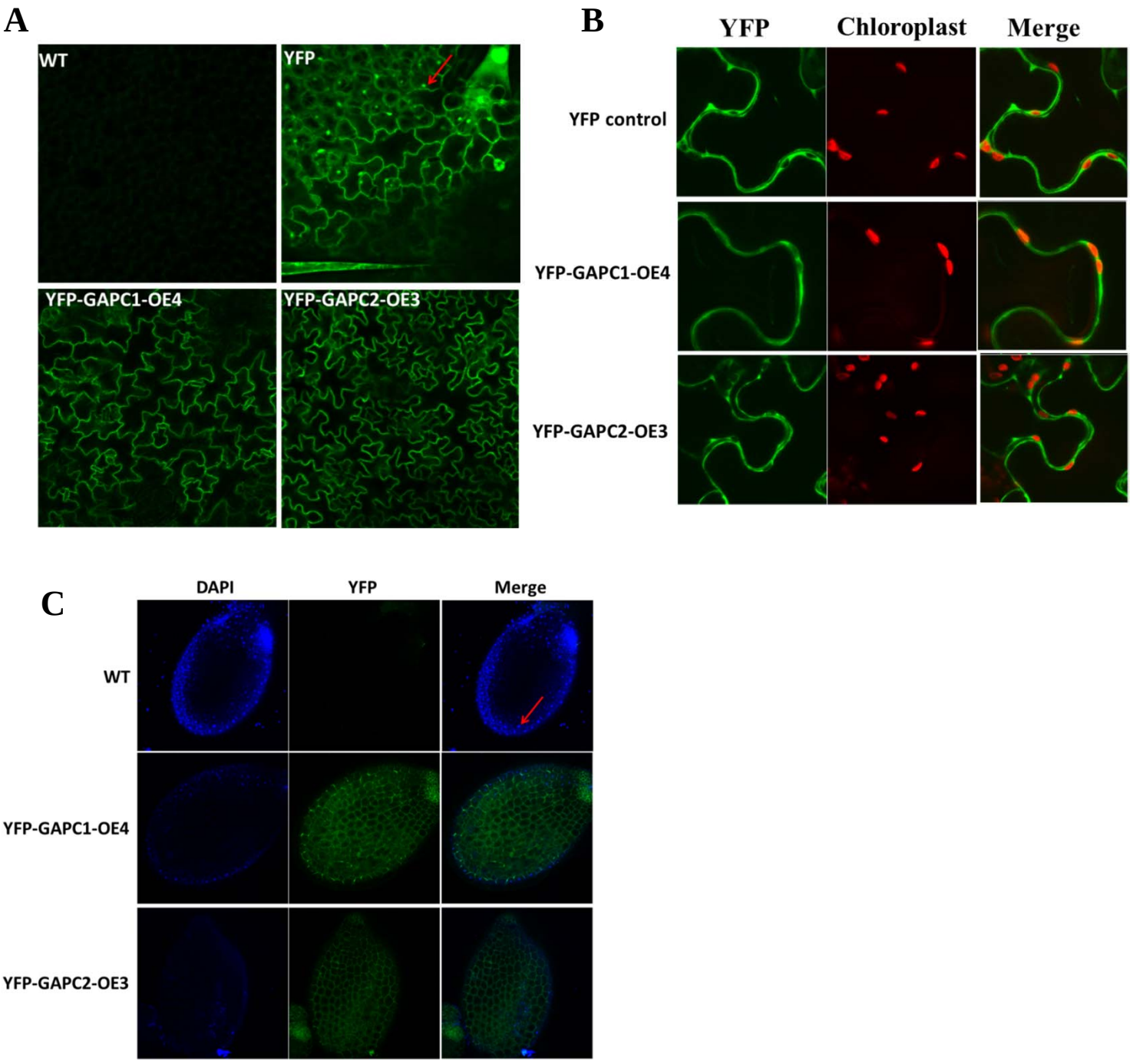

Supplemental Figure 2. Subcellular localization of *GAPC*.
(A) Expression of YFP-GAPC in Arabidopsis leaves. YFP-GAPC1 and YFP-GAPC2 were highly expressed in leaves. YFP was used as control and indicated nucleus localization in some cells while YFP-GAPCs did not have significant nucleus accumulation (indicated by red arrow). Green color represents YFP fluorescence.
(B) YFP-GAPC1 and YFP-GAPC2 both mainly localized in cytosol in leaves. Green color represents YFP fluorescence and red color marks chloroplasts as a reference.
(C) Expression of YFP-GAPC1 and YFP-GAPC2 in developing seeds (4 DAF). Seeds were stained by 4`,6-diamidino-2-phenylindole (DAPI, blue) to show nucleus (indicated by red arrow).

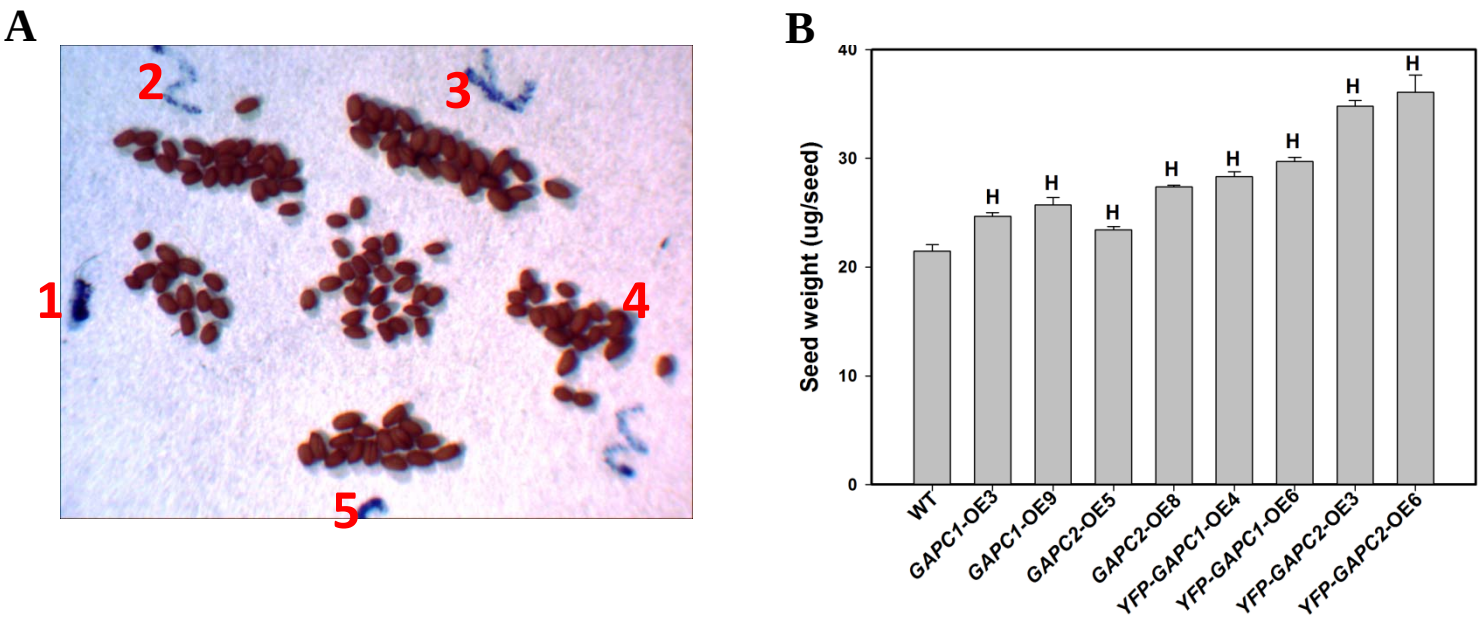

Supplemental Figure 3. Overexpression **(**OE) of *GAPC*s under the control of 35S promoter resulted in bigger and heavier seeds.

(A) Photo of seeds was taken under microscope. WT seeds are in the middle. 1, *YFP-GAPC1*-OE4; 2, *YFP-GAPC2*-OE6; 3, *YFP-GAPC2*-OE2; 4, *YFP-GAPC2*-OE3; 5, *YFP-GAPC2*-OE6.

(B) Seed weight of WT and 35S promoter-driven *GAPC* OE seeds. Seed weight was average weight based on calculation of the total weight (~3 mg) and total number of seeds. Values are means ± SD (n = 3). H indicates significantly higher than WT (student *t*-test, $P < 0.05$).

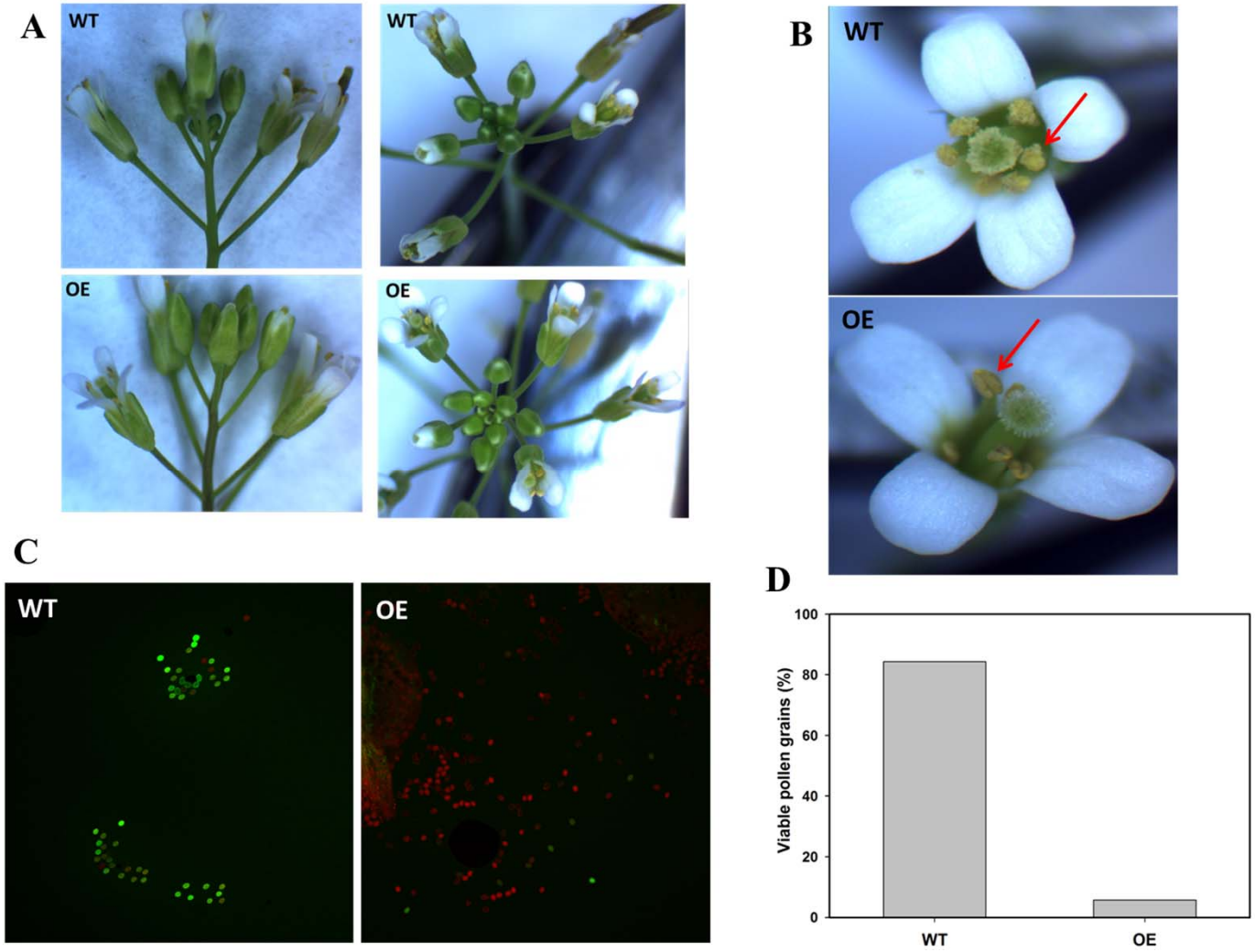

Supplemental Figure 4. OE of *GAPC*s under the control of 35S promoter causes male sterility.
(A) Morphology of WT and OE flowers under microscope.
(B) Flowers of WT and OE under microscope. Pollen could be observed on the WT anther after dehiscence (2 days after flowering). Anther of OE did not dehisce and no pollen were on the anther after flowering.
(C) Pollen viability staining by fluorescein diacetate (green) and propidium iodide (red). Green indicated viable pollen and red indicated dead pollen. Pollen from OE flower was obtained by manually disruption of the anther locules.
(D) Percentage of viable pollen in WT and OE.

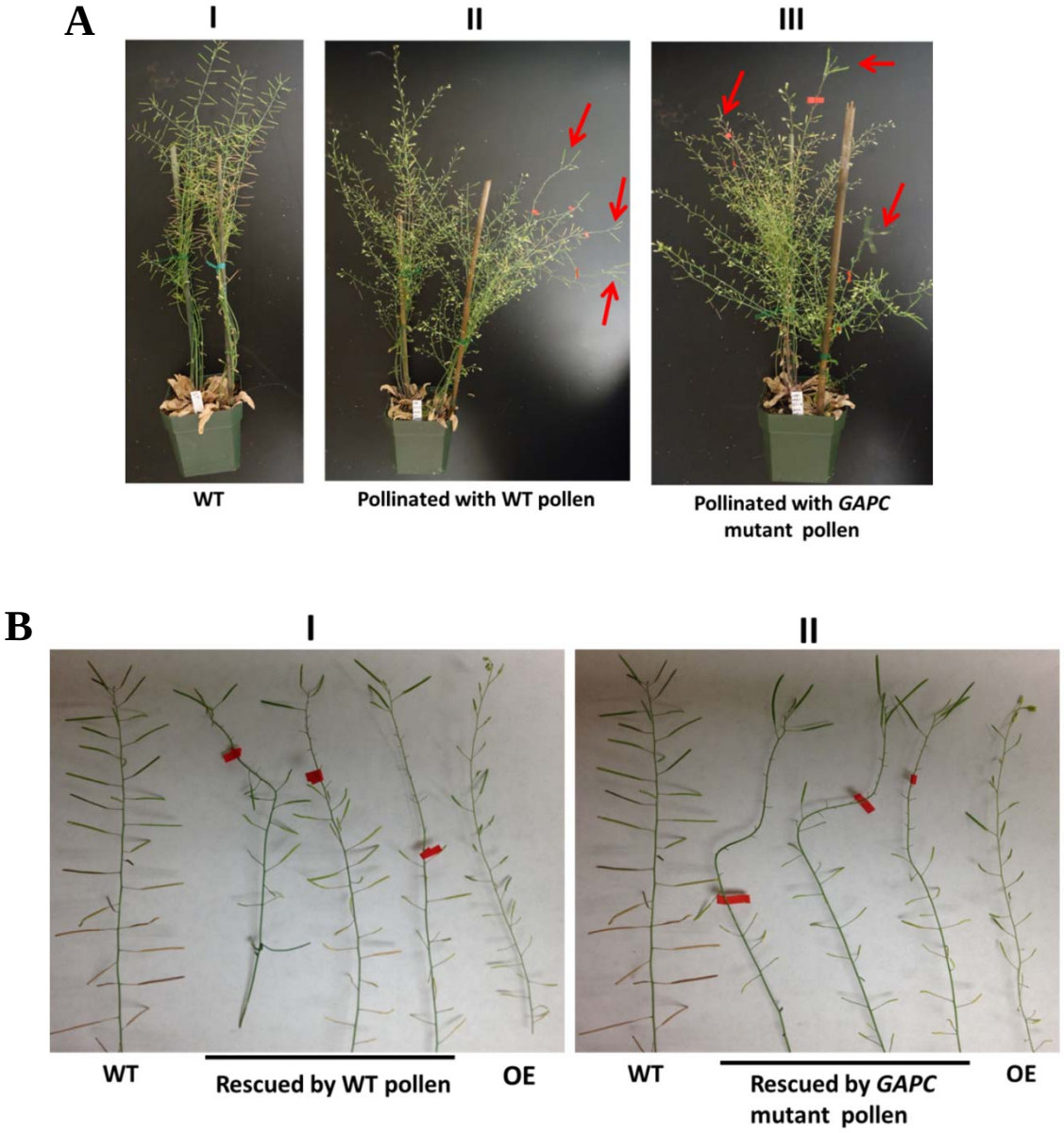

Supplemental Figure 5. Both WT and *gapc1-1 gapc2-1* pollen rescued silique development of 35S promoter-driven OE plants.
(A) Fertilize stigma of OE flower (anther removed before opening) with WT pollen or *gapc1-1 gapc2-1* pollen rescued silique development of OE plants. I, WT; II, *YFP-GAPC2* OE, red arrow indicates formation of normal siliques after flower pollinated with WT pollen; III, *YFP-GAPC2* OE, red arrow indicates formation of normal siliques after flower pollinated with *gapc1-1 gapc2-1* pollen.
(B) Comparison of siliques between WT, rescued OE and *YFP-GAPC2* OE. In I and II, only the top 3 siliques on each stem were normally formed because of fertilization by WT or *gapc1-1 gapc2-1* pollen, indicates the pollen of OE plants can't fertilize the stigma.

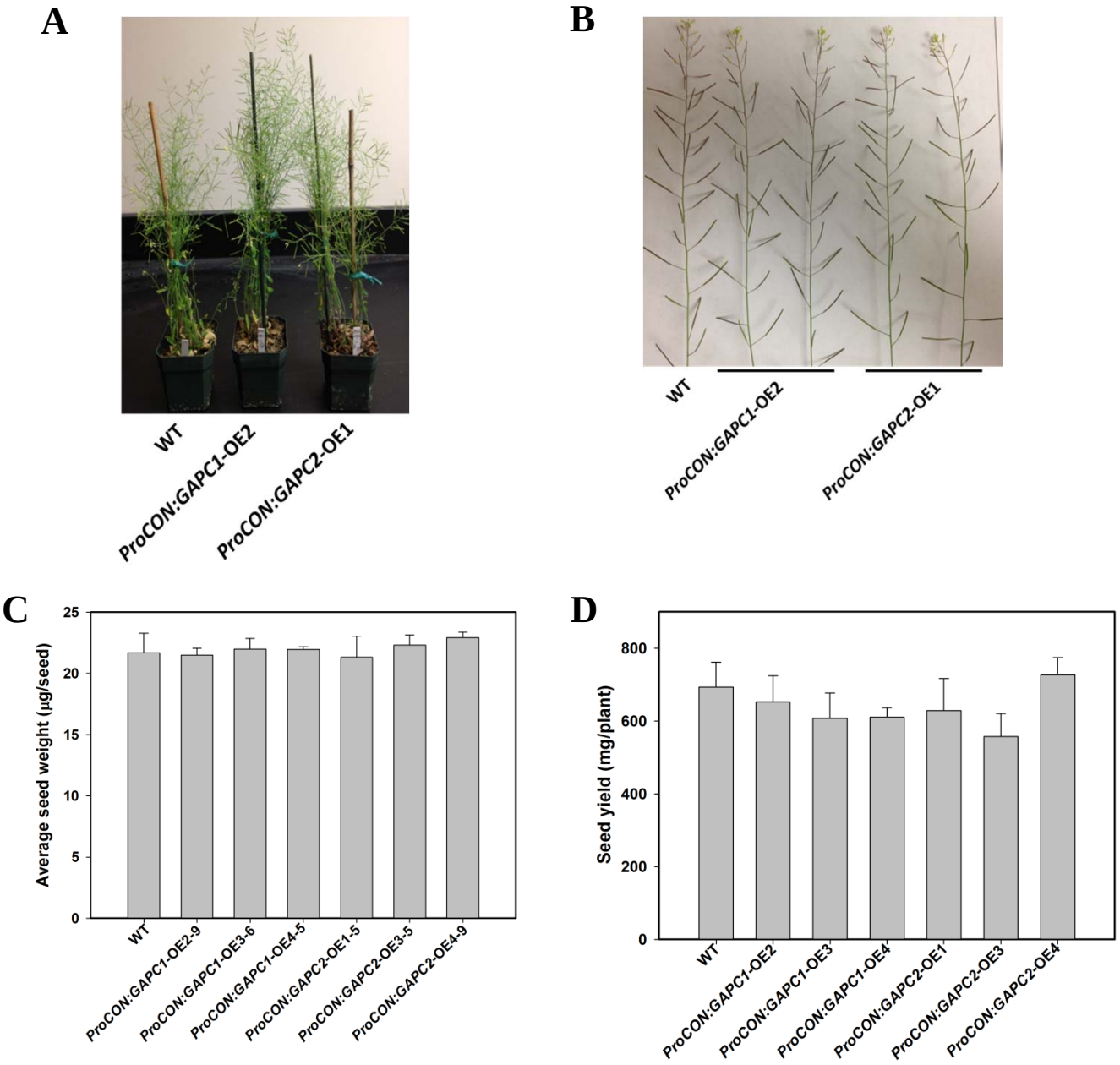

Supplemental Figure 6. Siliques develop normally on plants of seed-specific OE of *GAPC*.
(A) Plants were 7 weeks old growing under 16 h light/ 8 h night.
(B) Silique development of *GAPC* seed-specific OE plants was as normal as WT.
(C) Seed weight of WT and seed-specific OE seeds. Seed weight was average weight based on calculation of the total weight (~3 mg) and total number of seeds. Values are means ± SD (n = 3).
(D) Seed yield per plant of WT and OE plants. Values are means ± SE (n = 8).

6

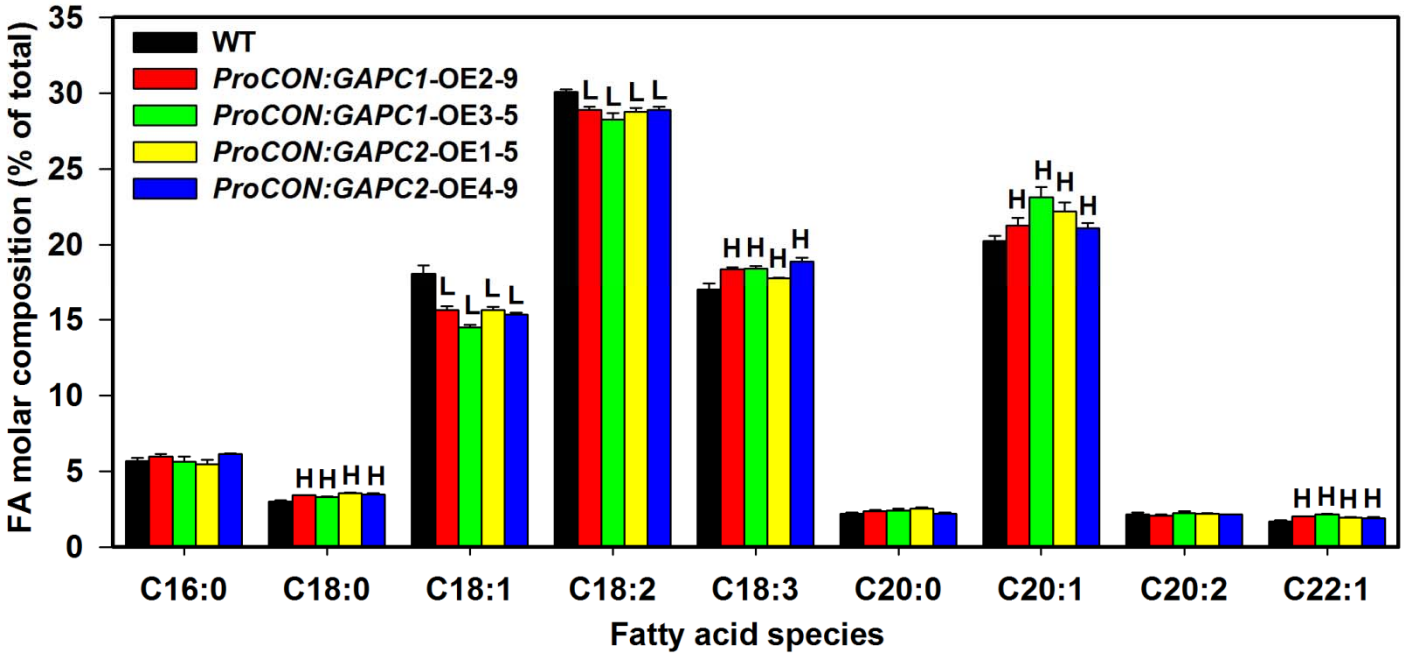

Supplemental Figure 7. Seed-specific OE of *GAPC*s alters fatty acid composition in the seeds.
Fatty acid composition was calculated as mol%. Values are means ± SD (n = 3). H and L indicate significantly higher and lower than WT (Student's *t*-test, $P < 0.05$).

7

Supplemental Table 1. Metabolites involved in the pentose phosphate pathway and starch biosynthesis pathway

Metabolite	WT	*gapc1-1gapc2-1*	GAPC1-OE#2	GAPC2-OE#1
Ribose-5-phosphate	13.77 ± 1.05^{a}	13.63 ± 0.63^{a}	10.89 ± 1.23^{a,b}	10.94 ± 0.89^{b}
Ribulose-5-phosphate	9.91 ± 1.24^{a}	10.49 ± 0.90^{a}	6.98 ± 1.09^{a}	7.52 ± 1.01^{a}
Xylulose-5-phosphate	22.95 ± 0.89^{a}	24.67± 1.82^{a}	18.48 ± 2.32^{a}	20.71 ± 2.94^{a}
Sedoheptulose-7-phosphate	80.4 ± 6.37^{a}	57.13 ± 9.17^{b}	65.54 ± 6.57^{a,b}	71.80 ± 6.87^{a,b}
Ribulose-1,5-bisphosphate	17.67 ± 2.22^{a}	12.11 ± 1.21^{b}	10.28 ± 1.66^{b,c}	7.64 ± 0.71^{c}
UDP	14.68 ± 1.65^{a,b}	11.46 ± 0.53^{b}	16.49 ± 1.56^{a}	18.10 ± 0.79^{a}
UDP-glucose	506.88 ± 15.07^{b}	415.98 ± 10.29^{c}	567.17 ± 56.69^{a,b}	673.87 ± 64.97^{a}

Values are means ± SE (n = 4). One-way ANOVA was performed and different lower case letters mark significant difference between means ($P < 0.05$).

Supplemental Table 2. Primer list

Purpose	Gene	ID	Primer name	Sequence
Gene cloning	GAPC1	At3g04120	GAPC1-F	GCGTTAATTAACATGGCTGACAAGAAGATTAGG
			GAPC1-R	GCG GTCGACTTAGGCCTTTGACATGTGGACGAT
Gene cloning	GAPC2	At1g13440	GAPC2-F	GCGTTAATTAACATGGCTGACAAGAAGATCAGA
			GAPC2-R	GCG GTCGACTTAGGCCTTTGACATGTGA
Gene cloning	GAPC1	At3g04120	ConGAPC1-F	GCGCGGCCGCACCATGGCTGACAAGAAGATTAGG
			ConGAPC1-R	GCGCGGCCGCTTATTTGTCGTCGTCGTCCTTGTAGTCCATGGCCTT
Gene cloning	GAPC2	At1g13440	BetaConGAPC2-F	GCGCGGCCGCACCATGGCTGACAAGAAGATCAGA
			BetaConGAPC2-R	GCGCGGCCGCTTATTTGTCGTCGTCGTCCTTGTAGTCCATGGCCTT TGACATGTGA
Real-time PCR	LPAAT1	At4g30580	AT1G15080.1_F	TGGTCAAAGAGGGACACAAGAGC
			AT1G15080.1_R	TCCTAGACCAGCAAACGACCAAG
Real-time PCR	LPAAT2	At3g57650	AT3G57650.1_F	TCAAAGGACAACCTTCAGTGGTG
			AT3G57650.1_R	ACCACTGTGCAATTGCGTCATC
Real-time PCR	LPAAT3	At1g51260	AT1G51260.1_F	GGCTCATCGTCAACATCATTCAGC
			AT1G51260.1_R	CAAGCCCACCAATCAAACAACC
Real-time PCR	LPAAT4	At1g75020	AT1G75020.1_F	TCCCTGAAGGAACCGATTTCACTG
			AT1G75020.1_R	ACGTTTGATAGTGCTGGAAGACC
Real-time PCR	LPAAT5	At3g18850	AT3G18850.1_F	AGGAGATGGGAAGTCGATGAAGC
			AT3G18850.1_R	TCCTTTGGCATTTAGCCTCTGTG
Real-time PCR	LPP1	At2g01180	AT2G01180.1_F	ATTCTGGCGCAATTCTCAGGAC
			AT2G01180.1_R	CGTGCTTGTGTTTAGAAGCGACTC
Real-time PCR	LPP2	At1g15080	AT4G30580.1_F	GGTCGCATTTCTAATGGCATGACG
			AT4G30580.1_R	TTCACTCGGGACAGCATGAAGG
Real-time PCR	LPP3	At3g02600	AT3G02600.1_F	TTCCAAGTGGACACACGTCATGG
			AT3G02600.1_R	GCTTTGCAACGTGGCCTTTACC
Real-time PCR	DGAT1	At2g19450	AT2G19450.1_F	TCGCTCCCACATTGTGTTATCAGC
			AT2G19450.1_R	AAATTGACGAGCCACCCAACCC
Real-time PCR	DGAT2	At3g51520	AT3G51520.1_F	TCCAGCCTAATCGTGCCTATGTC
			AT3G51520.1_R	AGCAACAACTCCAATCGGTAGCAC
Real-time PCR	PDAT1	At5g13640	AT5G13640.1_F	AAAGGATGTTGCAGTTGCCAGAG
			AT5G13640.1_R	TGTTGAGTCCCATGTGCGTGTC
Real-time PCR	PDAT2	At3g44830	AT3G44830.1_F	AGATGATGAGACGAGCCGAAGC
			AT3G44830.1_R	TCTCTGGTGCCTCCGGTAATTTG
Real-time PCR	CCT1	At2g32260	AT2G32260.1_F	AGGAGTTTCTTGACAAGCACCAG
			AT2G32260.1_R	AGCTCCGCTTGAATCAGCATAGG
Real-time PCR	CCT2	At4g15130	AT4G15130.1_F	TCCAGATGCACCATGGGTTCTTAC
			AT4G15130.1_R	AGCTCCACTAGTATCCGCATAGGG
Real-time PCR	AAPT1	At1g13560	AT1G13560.1_F	AGTTGGGTGCCATTTGTGAATGAG
			AT1G13560.1_R	TGCTCCCGTTTCTTGATCGAACG
Real-time PCR	AAPT2	At3g25585	AT3G25585.1_F	TCCTCTGCTGATTCTTCGCTGAC
			AT3G25585.1_R	TTGGGTCTCTCTCAAATCAACGAC
Real-time PCR	UBQ10	At4g05320	AT4G05320.1_F	CACACTCCACTTGGTCTTGCGT
			AT4G05320.1_R	TGGTCTTTCCGGTGAGACTCTTCA